

# Threshold Voltage Modeling of Double-Gate MOSFETs by Considering Barrier Lowering

Byung-Kil Choi, Ki-Heung Park, Kyoung-Rok Han, Young Min Kim, and Jong-Ho Lee

**Abstract**—Threshold voltage ( $V_{th}$ ) modeling of double-gate (DG) MOSFETs was performed, for the first time, by considering barrier lowering in the short channel devices. As the gate length of DG MOSFETs scales down, the overlapped charge-sharing length ( $x_h$ ) in the channel which is related to the barrier lowering becomes very important. A fitting parameter  $\delta_w$  was introduced semi-empirically with the fin body width and body doping concentration for higher accuracy. The  $V_{th}$  model predicted well the  $V_{th}$  behavior with fin body thickness, body doping concentration, and gate length. Our compact model makes an accurate  $V_{th}$  prediction of DG devices with the gate length up to 20-nm.

**Index Terms**—Barrier lowering, Bulk FinFET, double-gate, modeling, threshold voltage

## I. INTRODUCTION

According to the projection of the 2007 International Technology Roadmap for Semiconductors (ITRS), the physical gate length of MOSFET for a microprocessor unit (MPU) can be scaled down to 18 nm in 2010 [1]. The scaling-down of devices is strongly required to achieve high integration density and performance.

Recently, bulk FinFETs have been considering very promising candidate for next generation memory cell transistors to be applicable to dynamic random access memory (DRAM) and flash memory [2]. As the gate length of bulk FinFETs [3]-[5] scales down, barrier lowering occurs in spite of low drain bias ( $V_{DS}=0.05$  V) because the depleted charge-sharing length ( $x_h$ ) [6] by

source and drain in short channel is overlapped. To apply the devices to integrated circuits, it is strongly required to model threshold voltage ( $V_{th}$ ) considering the barrier lowering in short channel. However, the  $V_{th}$  model has not been developed since the  $x_h$  modeling in short channel devices is very complicated with device geometry and doping concentration. For  $V_{th}$  modeling of the devices, double-gate (DG) nature is key point and needs to be understood well.

In this paper, we propose  $V_{th}$  model of DG MOSFETs [7], [8] based on the correction of  $x_h$  considering barrier lowering, and verify the  $V_{th}$  model by comparing with device simulation [9] in terms of gate length ( $L_g$ ), fin width ( $W_{fin}$ ) and body doping ( $N_b$ ). Threshold voltages were extracted by using  $g_{m,max}$  for a given  $V_{DS}$  of 0.05 V in this paper.

## II. DEVICE STRUCTURE

Fig. 1 shows 3-D schematic view of the bulk FinFET. The  $H_g$  and  $W_{fin}$  represent gate height and fin width, respectively. The  $x_{jSDE}$  stands for junction depth of

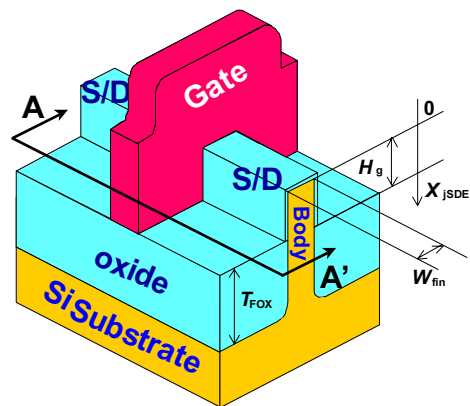


**Fig. 1.** 3-D schematic view of bulk FinFET. The  $H_g$  and  $W_{fin}$  represent fin height and width, respectively.

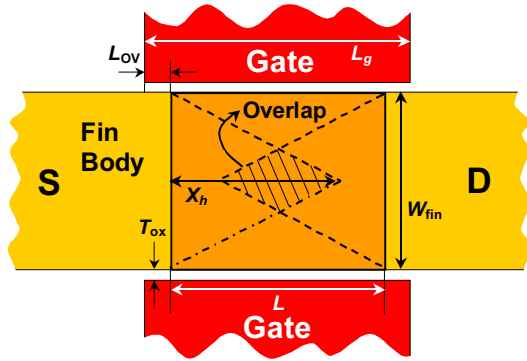


**Fig. 2.** 2-D cross-sectional view of the bulk FinFET along A-A' in Fig. 1. The  $T_{ox}$  and  $x_h$  represent gate oxide thickness and charge-sharing length, respectively.

source/drain extensions (SDE). The SDE concentration is  $7 \times 10^{19} \text{ cm}^{-3}$  and has the profile of about dec/5 nm. Gate oxide thickness ( $T_{ox}$ ) is fixed at 1.5 nm.  $T_{FOX}$  represents field oxide thickness for device isolation.

Fig. 2 shows 2-D schematic view of the DG MOSFET. Channel doping is uniform and a variable.  $n^+$  poly gate was applied.

### III. $V_{TH}$ MODEL AND VERIFICATION

Fig. 3 shows  $\delta_w$  versus  $W_{fin}$  as a parameter of the body doping. Here, the  $\delta_w$  [10] is a fitting parameter representing a difference between  $V_{th,simulation}$  and  $V_{th,model}$ , and introduced to take into account the  $V_{th}$  change with the  $W_{fin}$ . A fitting parameter  $\delta_w$  (empirical) is given by a kind of empirical equation based on various data. In Fig. 3, the empirical model (open symbols) shows a good agreement with the fitted data (solid symbols), and is given by

$$\begin{aligned} \delta_w = & \left( -0.04461 - 0.00354 \cdot \frac{N_b}{10^{18}} + 0.22176 \times 0.2564 \frac{N_b}{10^{18}} \right) \\ & + \left( 0.00322 + 0.00008 \cdot \frac{N_b}{10^{18}} - 3.50807 \times 0.0171 \frac{N_b}{10^{18}} \right) W_{fin} \\ & + \left( -0.00006 + 0.000006 \cdot \frac{N_b}{10^{18}} + 0.00733 \times 0.0618 \frac{N_b}{10^{18}} \right) W_{fin}^2. \end{aligned} \quad (1)$$

In Fig. 2, as the  $L_g$  of the device scales down, the  $x_h$ s from the source and the drain are overlapped each other. The overlap of  $x_h$  means barrier lowering, and affects  $V_{th}$  behavior. Therefore, the  $V_{th}$  model of DG MOSFETs must be modified by taking into account barrier lowering

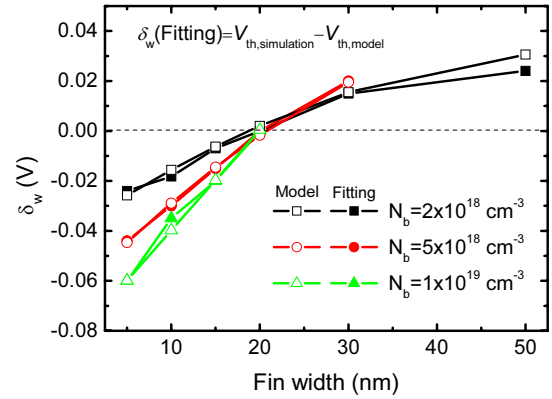


**Fig. 3.**  $\delta_w$  versus fin width as a parameter of the body doping. The  $\delta_w$  is obtained by subtracting the modeled  $V_{th}$  from the simulated  $V_{th}$ .

in  $x_h$  of short channel DG devices. To see an internal physics for the 20 nm device, we prepared Fig. 4 which shows the conduction band energy diagrams cut along the channel width direction at a point showing peak conduction band energy over the channel length at given  $V_{DS}=0.05 \text{ V}$  and  $V_{GS}=V_{th}$  condition. It is normal that the conduction band minimum is found at the channel surface in a device without barrier lowering. However, the 20 nm DG devices show the minimum point of the conduction band at the center of the body due to the barrier lowering. In Fig 5, we observe the conduction band energy starts to decrease when  $L_g$  decreases from 50 nm to 40 nm for given  $N_b$  of  $2 \times 10^{18} \text{ cm}^{-3}$  and  $W_{fin}$  of 15 nm. This change corresponds exactly to the  $x_h$  overlap represented by dotted line in Fig. 9. The devices in both Figs. 5 and 9 have the same device geometry and body doping. Since the  $x'_h (=x_h - \Delta x_h)$  which is charge-sharing length considering barrier lowering is function of  $N_b$ ,  $W_{fin}$ , and  $L_g$ , it is very difficult (or complicated) to derive an equation of  $x'_h$  based on physics. We performed device simulation extensively by changing 3 parameters mentioned above. Then we obtained a sort of empirical equation at a fixed  $N_b$  to explain  $x'_h$  for given  $W_{fin}$  and  $L_g$  by fitting the equation to the ( $x'_h$ )s extracted from simulated data. As an example, an empirical  $x'_h$  for an  $N_b$  of  $2 \times 10^{18} \text{ cm}^{-3}$  and  $L_g$  of 20 nm to 40 nm is given by

$$\begin{aligned} x'_h = & (8.31586 + 0.52656 \cdot L_g - 0.01177 \cdot L_g^2) - (0.0401 + 0.00258 \cdot L_g \\ & - 0.00021 \cdot L_g^2) \cdot W_{fin} - (69.14274 - 4.86237 \cdot L_g + 0.0389 \cdot L_g^2) \\ & \times (1.23917 - 0.02648 \cdot L_g + 0.0004 \cdot L_g^2)^{W_{fin}}. \end{aligned} \quad (2)$$

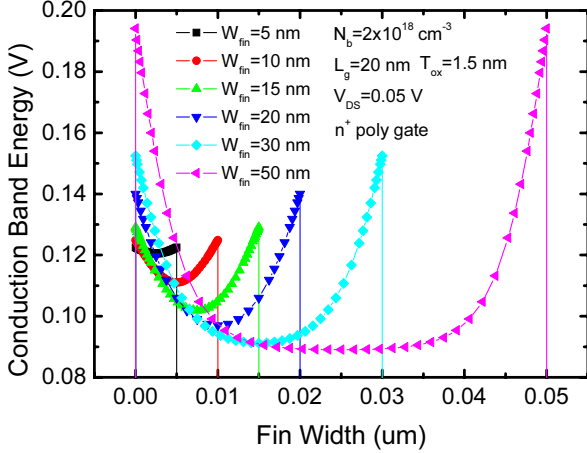


**Fig. 4.** Conduction band energy versus fin width as a parameter of  $W_{fin}$ . This figure shows conduction band energy diagrams cut along the channel width direction at a point showing peak conduction band energy over the channel length at  $V_{DS}=0.05$  V and  $V_{GS}=V_{th}$  condition.

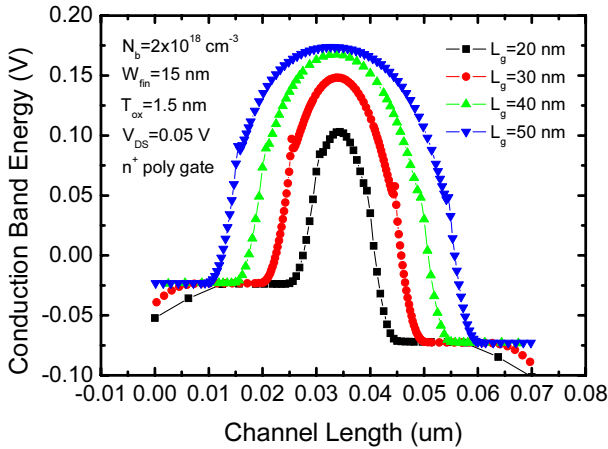


**Fig. 5.** Conduction band energy versus channel length as a parameter of  $L_g$ . This figure shows conduction band energy diagrams cut along the channel length direction in the center of fin body at  $V_{DS}=0.05$  V and  $V_{GS}=V_{th}$  condition.

The empirical ( $x'_h$ )s for an  $N_b$  of  $5 \times 10^{18} \text{ cm}^{-3}$  was also obtained by the same manner. Empirical equation (2) and  $x'_h$  extracted from the simulated data are compared in Fig. 7 which shows  $x'_h$  versus  $W_{fin}$  as a parameter of  $L_g$  for the devices with  $N_b$ s of  $2 \times 10^{18} \text{ cm}^{-3}$  and  $5 \times 10^{18} \text{ cm}^{-3}$ . The  $V_{th}$  model of ideal DG bulk FinFETs was already derived by B-K. Choi *et al.* [6]. We took  $V_{th}$  model reflecting only DG nature, and changed charge-sharing term by considering barrier lowering as given by

$$V_{th} = V_{FB} + 2\psi_B + \delta_w + \frac{qN_b x_{dep}}{C_{ox}} \left( 1 - \frac{x'_h}{L_c} \right) \quad (3)$$

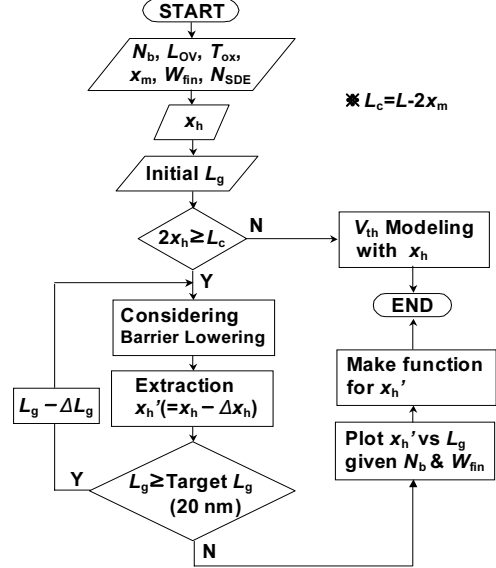


**Fig. 6.** Procedure of  $V_{th}$  modeling and extraction of charge-sharing length ( $x'_h$ ) depending on  $L_g$  for a DG MOSFET. Here,  $x_m$  is a parameter regarding box type channel doping and is calculated for a channel doping profile.

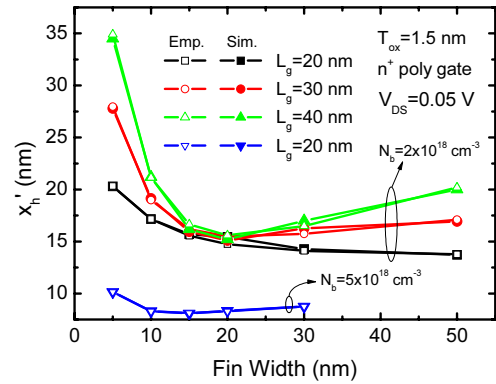


**Fig. 7.**  $x'_h$  versus  $W_{fin}$  as a parameter of  $L_g$  for the devices with  $N_b$ s of  $2 \times 10^{18} \text{ cm}^{-3}$  and  $5 \times 10^{18} \text{ cm}^{-3}$ . The empirical equations (open symbols) show a good agreement with ( $x'_h$ )s from simulation (solid symbols).

where  $x_{dep}$  is a depletion width, and  $0.5 \cdot W_{fin}$  if the fin body is depleted fully. The  $V_{FB}$ ,  $2\psi_B$  and  $C_{ox}$  are workfunction difference, surface potential at  $V_{th}$ , and gate oxide capacitance, respectively. We ignore oxide charge in this paper to simplify the modeling and simulations.

Fig. 6 shows the procedure of  $V_{th}$  modeling and extraction of suitable charge-sharing length ( $x'_h$ ) depending on  $L_g$  at a given  $N_b$  and  $W_{fin}$  for DG MOSFETs. Here,  $L_c (= L - 2x_m)$  [6] is the channel length based on the box channel doping profile.  $L_{ov}$  is shown in Fig. 2.

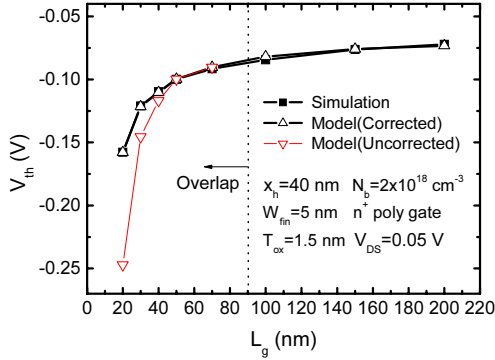


**Fig. 8.**  $V_{th}$  versus  $L_g$ . Here,  $W_{fin}$  of 5 nm and  $N_b$  of  $2 \times 10^{18} \text{ cm}^{-3}$  are applied. The overlap of  $x_h$  occurs at  $L_g$  of 90 nm. The model(Corrected) shows a good agreement with 2-D device simulation.

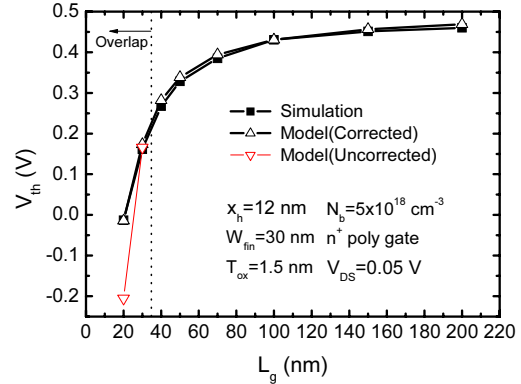


**Fig. 11.**  $V_{th}$  versus  $L_g$ . Here,  $W_{fin}$  of 30 nm and  $N_b$  of  $5 \times 10^{18} \text{ cm}^{-3}$  are applied. The overlap of  $x_h$  occurs at  $L_g$  of 35 nm. The model(Corrected) shows a good agreement with 2-D device simulation.

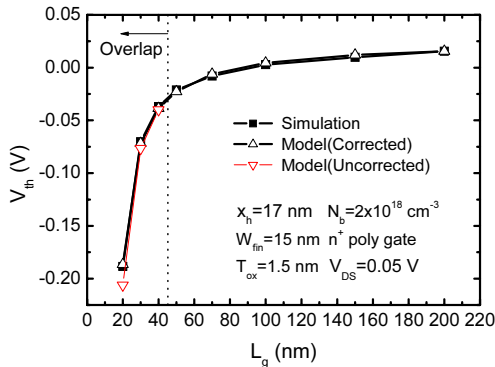


**Fig. 9.**  $V_{th}$  versus  $L_g$ . Here,  $W_{fin}$  of 15 nm and  $N_b$  of  $2 \times 10^{18} \text{ cm}^{-3}$  are applied. The overlap of  $x_h$  occurs at  $L_g$  of 45 nm. The model(Corrected) shows a good agreement with 2-D device simulation.

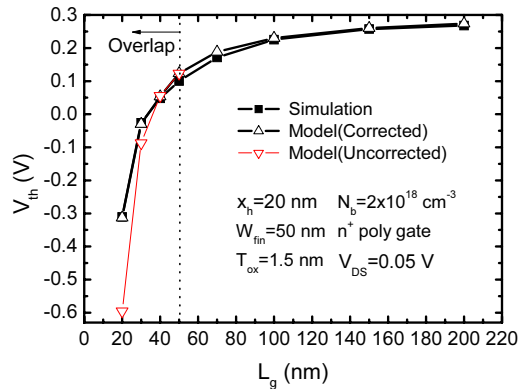


**Fig. 12.**  $V_{th}$  versus  $L_g$ . Here,  $W_{fin}$  of 50 nm and  $N_b$  of  $2 \times 10^{18} \text{ cm}^{-3}$  are applied. The overlap of  $x_h$  occurs at  $L_g$  of 41 nm. The model(Corrected) shows a good agreement with 2-D device simulation.

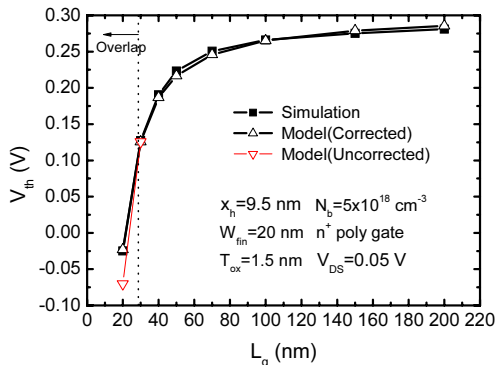


**Fig. 10.**  $V_{th}$  versus  $L_g$ . Here,  $W_{fin}$  of 20 nm and  $N_b$  of  $5 \times 10^{18} \text{ cm}^{-3}$  are applied. The overlap of  $x_h$  occurs at  $L_g$  of 29 nm. The model(Corrected) shows a good agreement with 2-D device simulation.

Figs. 8 – 12 show  $V_{th}$  versus  $L_g$  at given  $W_{fin}$  and  $N_b$ . In these figures, charge-sharing length is overlapped in the left side of the dotted line. The  $V_{th}$  model of DG MOSFETs with the uncorrected  $x_h$  shows some error with 2-D device simulation for various conditions in the

overlapped channel length. But the  $V_{th}$  model of DG MOSFETs with the corrected  $x_h$  shows a good agreement with 2-D device simulation regardless of  $L_g$ ,  $W_{fin}$ , and  $N_b$ .

#### IV. CONCLUSION

We have modeled threshold voltage ( $V_{th}$ ) of double-gate (DG) MOSFETs by considering barrier lowering in the short channel devices. The barrier lowering was reflected in charge-sharing length ( $x_h$ ) which was given by empirical equation including effects from fin body width and channel length. In  $V_{th}$  modeling, a fitting parameter  $\delta_w$  which is a kind of empirical equation based on various data was introduced for higher accuracy. The  $V_{th}$  model was verified by comparing with 2-D simulation data for various fin body width, gate length, and fin body doping. Our compact model explained well

the  $V_{th}$  behavior when charge-sharing length is overlapped.

### ACKNOWLEDGMENTS

This work was in part supported by “The National research program for the 0.1 Tb Non-volatile Memory Development sponsored by Korea Ministry of Science & Technology” in 2007.

### REFERENCES

- [1] International Technology Roadmap for Semiconductors, 2007. [Online]. Available: <http://public.itrs.net>
- [2] Tai-Su Park, Hye Jin Cho, Jeong Dong Choe, Sang Yeon Han, Donggun Park, Kinam Kim, Euijoon Yoon, and Jong-Ho Lee, “Characteristics of the Full CMOS SRAM Cell Using Body-Tied TG MOSFETs (Bulk FinFETs),” *IEEE Trans. Electron Devices*, vol. 53, no. 3, pp. 481–487, Mar. 2006.
- [3] Tai-su Park, Euijoon Yoon, Jong-Ho Lee, “A 40nm body-tied FinFET (OMEGA MOSFET) using bulk Si wafer,” *Physica E*, vol. 19, no. 1, pp. 6–12, 2003.
- [4] T. Park, S. Choi, D. H. Lee, J. R. Yoo, B. C. Lee, J. Y. Kim, C. G. Lee, K. K. Chi, S. H. Hong, S. J. Hyun, Y. G. Shin, J. N. Han, I. S. Park, U I. Chung, J. T. Moon, E. Yoon, and J. H. Lee, “Fabrication of body-tied FinFETs (Omega MOSFETs) using bulk Si wafers,” in *Symp. on VLSI Tech. Dig.*, 2003, pp. 135–136.
- [5] T. Park, H. J. Choe, S. Y. Han, S.-M. Jung, B. Y. Nam, O. I. Kwon, J. N. Han, H. S. Kang, M. C. Chae, G. S. Yeo, S. W. Lee, D. Y. Lee, D. Park, K. Kim, E. Yoon, and J. H. Lee, “Static noise margin of the full DG-CMOS SRAM cell using bulk FinFETs (Omega MOSFETs),” in *IEDM Tech. Dig.*, Dec. 2003, pp. 27–30.
- [6] Byung-Kil Choi, Kyoung-Rok Han, Young Min Kim, Young June Park, and Jong-Ho Lee, “Threshold-Voltage Modeling of Body-Tied FinFETs (Bulk FinFETs),” in *IEEE Trans. Electron Devices*, vol. 54, no. 3, pp. 537–545, Mar. 2007.
- [7] Gulzar A. Kathawala, Brain Winstead and Umberto Ravaioli, “Monte Carlo simulation of double-gate MOSFETs,” *IEEE Trans. Electron Devices*, vol. 50, no. 12, pp. 2467–2473, Dec. 2003.
- [8] Qiang Chen, Evans M. Harrel and James D. Meindl, “A physical short-channel threshold voltage model for undoped symmetric double-gate MOSFETs,” *IEEE Trans. Electron Devices*, vol. 50, no. 7, pp. 1631–1637, July 2003.
- [9] SILVACO International, ATLAS User’s Manual, 2007. [Online]. Available: <http://www.silvaco.com>
- [10] Byung-Kil Choi, Young Min Kim, Kyoung-Rok Han, Young June Park, and Jong-Ho Lee, “Threshold Voltage Modeling of Bulk FinFETs by Considering Corner Effect,” in *Si Nanoelectronics Tech. Dig.*, 2006, pp. 67–68.



**Byung-Kil Choi** was born in Daegu, Korea in 1974. He received the B.S. degree and M. S. degree in Electronic and Electrical Engineering from Kyungpook National University, Korea, in 2001 and 2004, respectively. He is pursuing Ph.D degree at the same institution. His research interests include threshold voltage, mobility, and I-V modelings of bulk FinFETs.



**Kiheung Park** was born in Korea on January 24, 1978. He received the B.S. degree in Electronic and Electrical Engineering from Hongik University, Korea, in 2004, and the M. S. degree in electrical and electronic engineering in 2006 from Kyungpook National University, Daegu, Korea, , where he is currently working toward the Ph. D. degree from Kyungpook National University, Daegu, Korea. His research interests include nano-scale CMOS (Bulk FinFET, and Saddle MOSFET) devices simulation and modeling of Saddle MOSFET.



**Kyoung-Rok Han** received the B.S degree in electrical engineering in 2002 from Wonkwang University and M.S degree in electrical engineering in 2004 from Kyungpook National University, Daegu, Korea.

He is pursuing Ph.D degree at the same institution. His research interests include the nano-scale CMOS (bulk FinFETs) and flash memory application of the device structure.



**Young Min Kim** received the B.S. degree in chemical engineering from Kyungpook National University, Daegu, Korea, and the M.S. degrees from Korea Advanced Institute of Science and Technology (KAIST), Daejeon, Korea, and North Carolina State University (NCSU), Raleigh, USA. He is currently pursuing the Ph.D. degree in the guidance of Professor Jong-Ho Lee.

His research interest is in the simulation and fabrication of quantum wire transistor and NFGM (Nano Floating Gate Memory).



**Jong-Ho Lee** received the B.S. degree in electronic engineering from Kyungpook National University, Daegu, Korea, in 1987. He received the M.S. and Ph.D. degrees from Seoul National University, Seoul, in 1989 and 1993, respectively, all in

electronic engineering. In 1993, he worked on advanced BiCMOS process development at ISRC of Seoul National University as an engineer. In 1994, he joined the School of Electrical Engineering, Wonkwang University, Iksan, Chonbuk. Since 2002, he has been with Kyungpook National University, Daegu, where he is currently a Professor of electrical and computer engineering. From 1994 to 1998, he was with ETRI as an invited member of technical staff, working on deep submicron SOI devices, device isolation,  $1/f$  noise, and device mismatch characterization. From August 1998 to July 1999, he worked at MIT as a post-doctor, where he was engaged in the research on sub-100 nm double-gate CMOS devices. His research interests include sub-100 nm device technologies, device characterization and modeling for RF application, high performance IC design, and 3-D Microsystems including sensors. He has authored or coauthored over 71 journal papers and over 146 conference papers related to his research, and has been granted 36 patents in this area.